Dynamics of Growth and Form in Prebiotic Vesicles

Teresa Ruiz-Herrero
John A. Paulson School of Engineering and Applied Sciences, Harvard University, Cambridge, Massachusetts 02138, USA

Thomas G. Fai
Department of Mathematics, Brandeis University, Waltham, Massachusetts 02453, USA

L. Mahadevan*
John A. Paulson School of Engineering and Applied Sciences, Department of Physics, Department of Organismic and Evolutionary Biology, Harvard University, Cambridge, Massachusetts 02138, USA

(Received 10 January 2019; published 19 July 2019)

The growth, form, and division of prebiotic vesicles, membraneous bags of fluid of varying components and shapes is hypothesized to have served as the substrate for the origin of life. The dynamics of these out-of-equilibrium structures is controlled by physicochemical processes that include the intercalation of amphiphiles into the membrane, fluid flow across the membrane, and elastic deformations of the membrane. To understand prebiotic vesicular forms and their dynamics, we construct a minimal model that couples membrane growth, deformation, and fluid permeation, ultimately couched in terms of two dimensionless parameters that characterize the relative rate of membrane growth and the membrane permeability. Numerical simulations show that our model captures the morphological diversity seen in extant precursor mimics of cellular life, and might provide simple guidelines for the synthesis of these complex shapes from simple ingredients.

DOI: 10.1103/PhysRevLett.123.038102

It is likely that the first cells originated when a self-replicating biomolecule was separated from its environment by a permeable membrane barrier and both the biomolecule and the membrane were able to grow and replicate. Physical compartmentalization allowed for a separation of chemical environments, making way eventually for the specialization and competition between cells that is the basis for Darwinian evolution [1,2]. How these prebiotic cells could grow and divide without the complex machinery in extant cells remains a major open question in biology. Given the strong chemical and physical constraints on biomolecular replication, and membrane compartmentalization, growth, and dynamics, it is natural to expect that physicochemical processes are intimately tied to the evolvability of such states. Recent research on the ability of a biomolecule to replicate and transmit information has led to a consensus on a range of possible chemical replicators [3]. Independently, the physical properties of the external membrane barrier under growth and division have also been the subject of experimental studies [4,5]. However, the phase space of physical solutions for the growth and form of the prebiotic vesicles is difficult to grapple with owing to the range of spatiotemporal processes that need to be accounted for—from membrane growth and deformation to fluid permeation and ultimately division. Insight into the dynamics of membrane growth and replication may be gleaned by considering artificial lipid vesicles as well as naturally occurring L-form bacteria. Synthetic lipid vesicles composed of single-chain amphiphiles are considered to be representative of prebiotic conditions [6], as are L-forms, naturally occurring bacteria with genetic mutations that inhibit cell wall formation [7]. Both these systems have been experimentally shown to exhibit complex shapes and modes of growth; they can grow while maintaining their original spherical shape, by elongating into cigar shapes that eventually divide into two vesicles of the same size [8–11] [Fig. 1(a)], or by developing protrusions in the form of external buds [9,12,13] [Fig. 1(b)], internal buds [10,12] [Fig. 1(d)], or long tubes [4,9,12–14] [Fig. 1(c)]. It has been suggested previously that growth and division may be controlled solely by the physical processes at play [5,15,16]. In particular, it is well established that deformations during growth involve dynamical imbalances in the surface area to volume ratio, either due to excess membrane growth or low permeability [13,17,18]. Our work builds on existing theoretical studies of the equilibrium shapes of vesicles [19–23] and out-of-equilibrium membrane growth [24–29] by exploring the range of possible behaviors within a nonequilibrium physical model that couples membrane growth and fluid permeation.

Our minimal model of prebiotic vesicles assumes a closed elastic surface of initial radius R_0, spontaneous curvature c_0, bending stiffness B, and fluid permeability K, with the membrane thickness being much smaller than the

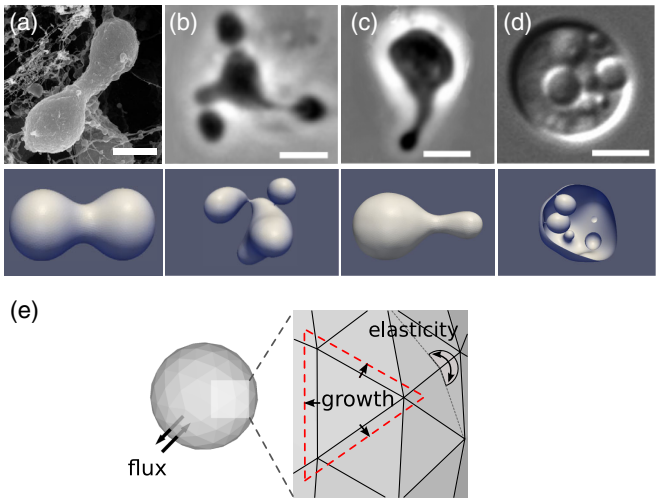

FIG. 1. (top) Different morphologies observed during growth in synthetic giant vesicles and L-form bacteria: (a) symmetric division, adapted from Ref. [11], (b) budding adapted from Refs. [10,13], (c) tubulation adapted from Ref. [13], (d) vesiculation adapted from Refs. [10,13] (Scale bars represent 3 μm). Our minimal model leads to shapes that are similar to those observed experimentally, using the following dimensionless parameters: (a) $\Pi_1 = 0.01$, $\Pi_2 = 2.5$, (b) $\Pi_1 = 0.15$, $\Pi_2 = 5$, (c) $\Pi_1 = 0.02$, $\Pi_2 = 5$, and (d) $\Pi_1 = 0.15$, $\Pi_2 = -2.5$ (see text for details). (e) A schematic of our vesicle model that uses a 3D triangulated lattice with bending rigidity B immersed in a fluid with viscosity μ, with area that grows with homogeneous expansion of the triangle size at a rate γ and volume whose evolution is controlled by the wall permeability K.

vesicle radius, which changes over time. We also assume the membrane to be nearly inextensible, which translates into a high energy cost for stretching, making bending deformations energetically preferable. The vesicle is assumed to be immersed in an incompressible fluid having viscosity μ and at temperature T. We further assume that the amphiphilic molecules that constitute the membrane are at a constant concentration in the surrounding medium and that they are incorporated into the membrane at an average net rate of γ. At a continuum level, this implies that the vesicle area A grows according to the simple law

$$\dot{A} = \gamma A. \tag{1}$$

Since lipids are incorporated into the external layer, we assume that rapid transbilayer lipid exchange distributes amphiphiles across the membrane and relaxes the bending energy [30], and further that amphiphile species determine the preferred spontaneous curvature [31]. We account for the vesicle permeability, with changes in the vesicle volume produced by transmembrane fluid flux according to

$$\dot{V} = AK\Delta P, \tag{2}$$

where the pressure drop $\Delta P = P_{\text{out}} - P_{\text{in}}$, and K is the membrane permeability. In this minimal model, we assume that the pressure drop is dominated by the osmotic component, which is kept constant by implicit internal mechanisms. We note that these two equations are incompatible with spherical vesicle growth, since they specify two laws for radial expansion—one linear and another exponential. Naturally, the slower of these is rate limiting, and this leads to the complexity of shapes seen, as we will see shortly.

Since the size of the system ($\sim$10 μm) is larger than the scale over which thermodynamic fluctuations are relevant (and $B/k_BT \sim 10$), we neglect the role of thermal fluctuations. In terms of the five variables, the bending stiffness (B), growth rate (γ), dynamic viscosity (μ), effective permeability ($K\Delta P$), and spontaneous curvature (c_0), we construct three relevant length scales: the critical radius $R_i = K\Delta P/\gamma$, i.e., the radius below which vesicle growth is dominated by volume increase and above which is dominated by area growth, the mechanical relaxation length scale $R_x = (B/\gamma\mu)^{1/3}$, the size below which bending deformations are mechanically equilibrated, but above which they are still dynamically varying, and the length scale related to the spontaneous curvature c_0^{-1}. Using the following values for the viscosity $\mu = 0.8 \times 10^{-3}$ kg/m s, bending stiffness $B = 10\, k_BT = 4 \times 10^{-20}$ J [32], scaled permeability $K\Delta P = 10^{-7} - 10^{-5}$ m/s [33–36], growth rate $\gamma = 0.5$ s^{-1} [6], and spontaneous curvature $|c_0| = 10^6$–10^8 m^{-1} [37], we find that $R_i \sim [10^{-7}$–$10^{-5}]$ m, $R_x \sim [5 \times 10^{-8}, 20 \times 10^{-7}]$ m. This allows us to define two dimensionless parameters: $\Pi_1 = R_i/R_x \in [0.01, 1]$, which accounts for the ability of the vesicle to mechanically equilibrate under imbalances arising from growth beyond R_i, and $\Pi_2 = R_i c_0 \in [0.1, 100]$, which determines the relative magnitude of spontaneous vesicle curvature (noting that it can be negative or positive). A small value of Π_1 corresponds to a small critical radius and large relaxation length scales: this is the limit of slow growth in which vesicles evolve in a sequence of quasiequilibrated shapes. On the other hand, large values of Π_1 correspond to large critical radii and small relaxation length scales which allow only for local equilibration; this is the limit of nonequilibrium growth. The subset of values we consider corresponds to the regime of membrane-driven growth, which we reason is likely when simple cellular precursors are unlikely to have been able to sustain high osmotic pressures.

We use overdamped dynamics to model the vesicle as a porous elastic membrane immersed in an incompressible fluid. The elastic energy of the lipid bilayer is assumed to be equal to the sum of the local stretching energy, the Canham-Helfrich Hamiltonian [38,39], and a penalty term that tethers the volume of the vesicle to the target volume V_T, which is typically growing. This yields the expression for the energy

$$E = \frac{k_a}{2}\int_{S'}(J-1)^2 da' + \frac{B}{2}\int_{S}(H-c_0)^2 da + \frac{k_V}{2}(V-V_T)^2, \tag{3}$$

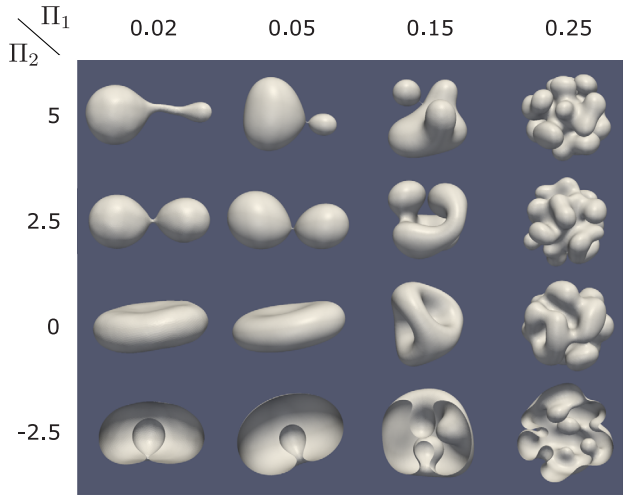

FIG. 2. Morphospace of vesicle shapes as a function of the dimensionless mechanical relaxation Π_1 and the dimensionless spontaneous curvature Π_2. For $\Pi_2 = -2.5$ the shapes also visualize the interior of the vesicles where vesiculation occurs. Configurations correspond to vesicle shapes immediately prior to division or fission, with snapshots of the vesicle just before a topological transition associated with fission.

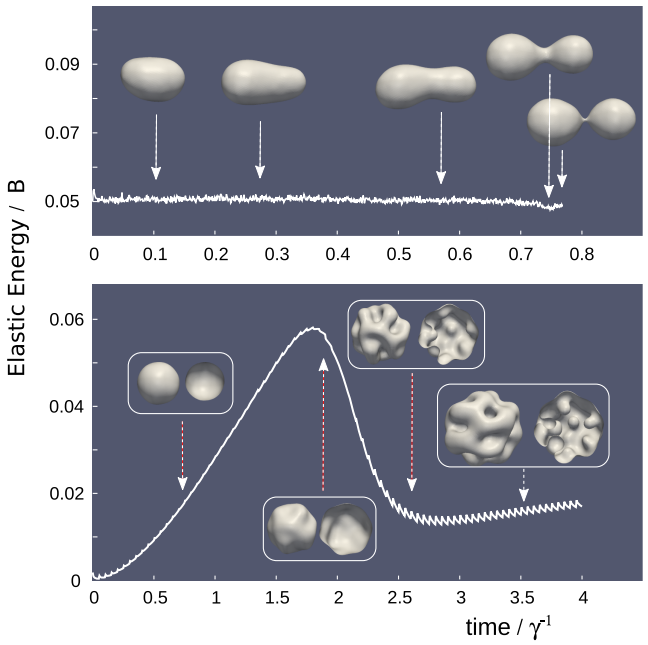

FIG. 3. Scaled elastic energy and vesicle shapes as a function of scaled time for two different modes of growth. (Top) When $\Pi_1 = 0.05$ and $\Pi_2 = 2.5$, the formation of a skinny neck between symmetric lobes provides a likely mechanism of homeostatic division in three dimensions. The slow growth allows the vesicle to deform through quasiequilibrated shapes with roughly constant elastic energy, and with a drop in the energy corresponding to neck formation. (Bottom) When $\Pi_1 = 0.25$ and $\Pi_2 = -2.5$, fast surface growth and negative curvature lead to multiple sites of inward vesiculation. The buildup in elastic energy is a signature of fast nonequilibrated growth. The shapes along the curve also show the interior of the vesicles.

where k_a is the stretching coefficient, B is the bending modulus, H is the sum of the principal curvatures, c_0 is the spontaneous curvature, and k_V is a volume-preserving penalty parameter. In the above integrals, da' is the area element in the reference surface $\mathbf{S}'$, da is the area element in the deformed configuration $\mathbf{S}$, and the term J that appears in the stretching energy is the Jacobian of the transformation from reference coordinates to deformed coordinates. The reference surface, i.e., the equilibrium state, is assumed to be a sphere, with the stretching term penalizing local changes in area relative to the reference configuration following Eq. (1), while the target volume follows Eq. (2). In our simulations, the membrane is represented as a triangulated lattice that undergoes growth and deformation [Fig. 1(e)], with vertices following Brownian dynamics in the presence of forces driven by the Hamiltonian above. To avoid numerical instabilities, the surface is remeshed periodically and the effective temperature is kept very small to ensure robustness with respect to mesh size and shape changes, and small fluctuations (see Supplemental Material [40] for further details).

We simulated vesicular growth using this model after initializing the vesicles as spheres with initial radius $R_0 = 2R_i$ over the range $\Pi_1 = 0.01$–0.5 and $\Pi_2 = -2.5$–5 by varying the growth rate, permeability, bending stiffness, and viscosity. First we study the shape evolution during growth as a function of Π_1 for vesicles with zero spontaneous curvature ($\Pi_2 = 0$ corresponding to the intermediate row of Fig. 2). In all our simulations reported in the Letter, we have chosen the stretching coefficient k_a to be sufficiently large so that bending, rather than in-plane stretching, is the preferred mode of deformation. We find a transition that occurs continuously around $\Pi_1 = 0.15$ with shapes showing increasingly high-order symmetries. Values of Π_1 below this transition correspond to quasiequilibrum shapes that continuously relax while the reduced volume decreases during growth [Fig. 3(a)]. Values of Π_1 above the transition correspond to nonequilibrated configurations in which surface growth is faster than the timescale for mechanical relaxation, so that the vesicle incorporates new material by corrugating its surface at the cost of increased elastic energy.

For the case of zero spontaneous curvature ($\Pi_2 = 0$), there is an energy barrier for neck formation that prevents budding or sprouting. Consequently, in the quasiequilibrated case the growing surface area can only be accommodated by the formation of vesicle-scale, pancakelike geometries. The most general way to form necks and thus take the simplest route to cell division, is by introducing a nonzero spontaneous curvature. Indeed, for fixed nonzero spontaneous curvature, with $\Pi_2 \neq 0$, we see the emergence of two different behaviors depending on the sign of the spontaneous curvature. Positive spontaneous curvatures give rise to tube formation and budding. Consistent with

the observations for $\Pi_2 = 0$, we observe quasiequilibrium shapes at small values of Π_1 in which a tube sprouts from the main body of the vesicle. As Π_1 is increased, tube formation is replaced by single budding events. At large values of Π_1, several budding sites emerge on the vesicle surface. Finally, negative spontaneous curvature corresponds to shapes with inner tubulation (small Π_1) and inner vesiculation [large Π_1, Fig. 3(b)]. In the Supplemental Material [40], we investigate the case of low k_a in which surface stretching becomes energetically preferable and find that rather than tube sprouting, a neck appears in the narrowest section of a pear-shaped vesicle (Supplemental Material [40]. Figure S1).

Large values of Π_1 correspond to the cases of high permeability and rapid growth, in which both vesicle volume and surface area grow faster than the timescale for mechanical relaxation, resulting in a buildup of elastic energy [Fig. 3(b)]. The vesicle grows spherically until volume growth cannot keep up with surface growth, at which point patches of constant mean curvature with $|c| \sim c_0$ appear throughout the surface to relax the bending energy. Further surface growth results in the accumulation of extra material in those patches, which subsequently become nucleation sites for budding or vesiculation.

Although we stop our simulations prior to vesicle fusion or division given the geometric and biophysical complexity of the topological transition associated with division in three dimensions, we can explore this process in the case of two dimensions (relevant for vesicles that are confined between solid surfaces) and also study the formation of thin necks Fig. 3(a), since this might lead to division spontaneously due to thermal fluctuations. Our qualitative exploration shown in Fig. 2 reveals various behaviors: we find vesicles approaching symmetric division with very small dispersion in size, and vesicles that develop small internal or external buds that might also be precursors to division. In this context, it is important to note that the initial radius influences the shape of the vesicles during growth. Assuming a spherical configuration and setting the radius change from the area and volume growth equations equal to each other, one may compute $R_c = 2K\Delta P/\gamma = 2R_i$ to be the radius at which volume growth cannot keep up with surface growth and the vesicle begins to deviate from a spherical shape. Whereas the above results were obtained using an initial vesicle radius of $R_0 = R_c$, if $R_0 < R_i$, there is a preliminary stage in which the vesicle grows spherically until reaching the critical radius R_c before the deformations discussed above occur. When $R_0 > R_c$ however, area growth is initially much faster than volume growth and the surface undergoes corrugations at lower values of Π_1; for large values of R_0, daughter vesicles will effectively bud off, reducing the radius of the mother vesicle until it reaches R_c.

Simulations in 2D systems (see Supplemental Material [40]), show very similar features that map onto the morphospace of Fig. 2, in the sense that vesicles will exhibit the morphologies of Fig. 2 immediately prior to division. Furthermore, in the 2D systems, we can capture the topological transitions associated with division easily and thus simulate multiple generations (see Ref. [40]). Vesicles that grow into cigar shapes display accurate size control when the permeability and growth rate are such that both the perimeter and area double simultaneously (Supplemental Material [40], Fig. S5), leading to a periodic steady state.

To assess the validity of our assumption of local hydrodynamics, we used the immersed boundary method [51] to model the nonlocal hydrodynamics and solved fthe fully coupled elastohydrodynamic problem (see the Supplemental Material [40]). While our results are qualitatively consistent with the simpler local hydrodynamic approximation used so far, accounting for nonlocal hydrodynamics increases the characteristic length scales of membrane tubules and invaginations and lowers the energy barrier for the formation of creases and folds (see Supplemental Material [40]).

Overall, our study of nonequilibrium vesicle growth and division allows us to investigate the role of permeability, stiffness, viscosity, and growth rate via two dimensionless parameters that define a two-dimensional morphospace. Our simulations reveal that many of the essential aspects of growth and dynamics can be understood in terms of an imbalance between surface to volume growth and the relative rate of mechanical relaxation. Our morphospace allows us to recapitulate the various observed shapes of simple dynamically growing lipid vesicles and their approximate biological analogs, *L*-forms [8–12], and allows us to evaluate whether the varied morphodynamics of prebiotic vesicles and their modern counterparts could arise from nonequilibrium physicochemical processes. Our minimal model provides a foundation to study the physicochemical constraints on protocellular growth and replication while setting the stage to include the additional complexity associated with the dynamics of transbilayer lipid exchange and natural curvature, internal sources of lipids, concentration differences across the membrane, and the role of multiple bilayers.

We thank Chris Rycroft, Charles Peskin, Chen-Hung Wu, and Etienne Vouga for useful discussions, and the Ramón Areces Foundation (T. R. H.), the National Science Foundation Grant No. DMS-1502851 (T. G. F.), and the Simons Collaboration on the Origins of Life 390237 (T. R. H. and L. M.) for partial support.

*Corresponding author.
Lmahadev@g.harvard.edu

[1] I. Budin and J. W. Szostak, Expanding roles for diverse physical phenomena during the origin of life, Annu. Rev. Biophys. **39**, 245 (2010).

[2] R. V. Solé, Evolution and self-assembly of protocells, Int. J. Biochem. Cell Biol. **41**, 274 (2009).
[3] P. G. Higgs and N. Lehman, The RNA World: Molecular cooperation at the origins of life, Nat. Rev. Genet. **16**, 7 (2015).
[4] T. F. Zhu and J. W. Szostak, Coupled growth and division of model protocell membranes, J. Am. Chem. Soc. **131**, 5705 (2009).
[5] I. Budin and J. W. Szostak, Physical effects underlying the transition from primitive to modern cell membranes, Proc. Natl. Acad. Sci. U.S.A. **108**, 5249 (2011).
[6] I. A. Chen and J. W. Szostak, A kinetic study of the growth of fatty acid vesicles, Biophys. J. **87**, 988 (2004).
[7] J. Errington, L-form bacteria, cell walls and the origins of life, Open Biol. **3**, 120143 (2013).
[8] R. Mercier, P. Domínguez-Cuevas, and J. Errington, Crucial role for membrane fluidity in proliferation of primitive cells, Cell Rep. **1**, 417 (2012).
[9] M. Leaver, P. Domínguez-Cuevas, J. M. Coxhead, R. A. Daniel, and J. Errington, Life without a wall or division machine in Bacillus subtilis, Nature (London) **457**, 849 (2009).
[10] F. O. Bendezú and P. A. J. de Boer, Conditional lethality, division defects, membrane involution, and endocytosis in mre and mrd shape mutants of Escherichia coli, J. Bacteriol. **190**, 1792 (2008).
[11] T. Onoda, J. Enokizono, H. Kaya, A. Oshima, P. Freestone, and V. Norris, Effects of calcium and calcium chelators on growth and morphology of Escherichia coli L-form NC-7, J. Bacteriol. **182**, 1419 (2000).
[12] P. Peterlin, V. Arrigler, K. Kogej, S. Svetina, and P. Walde, Growth and shape transformations of giant phospholipid vesicles upon interaction with an aqueous oleic acid suspension, Chem. Phys. Lipids **159**, 67 (2009).
[13] R. Mercier, Y. Kawai, and J. Errington, Excess membrane synthesis drives a primitive mode of cell proliferation, Cell **152**, 997 (2013).
[14] J. W. Szostak, An optimal degree of physical and chemical heterogeneity for the origin of life, Philos. Trans. R. Soc. B Biol. Sci. **366**, 2894 (2011).
[15] Y. Briers, T. Staubli, M. C. Schmid, M. Wagner, M. Schuppler, and M. J. Loessner, Intracellular vesicles as reproduction elements in cell wall-deficient L-form bacteria, PLoS One **7**, e38514 (2012).
[16] D. Zwicker, R. Seyboldt, C. A. Weber, A. A. Hyman, and F. Jülicher, Growth and division of active droplets provides a model for protocells, Nat. Phys. **13**, 408 (2017).
[17] J. Käs and E. Sackmann, Shape transitions and shape stability of giant phospholipid vesicles in pure water induced by area-to-volume changes, Biophys. J. **60**, 825 (1991).
[18] L. K. Harris, N. A. Dye, and J. A. Theriot, A Caulobacter MreB mutant with irregular cell shape exhibits compensatory widening to maintain a preferred surface area to volume ratio, Mol. Microbiol. **94**, 988 (2014).
[19] S. Svetina and B. Žekš, Membrane bending energy and shape determination of phospholipid vesicles and red blood cells, Eur. Biophys. J. **17**, 101 (1989).
[20] U. Seifert, Configurations of fluid membranes and vesicles, Adv. Phys. **46**, 13 (1997).
[21] A. J. Markvoort, R. Van Santen, and P. Hilbers, Vesicle shapes from molecular dynamics simulations, J. Phys. Chem. B **110**, 22780 (2006).
[22] B. Kaoui, A. Farutin, and C. Misbah, Vesicles under simple shear flow: Elucidating the role of relevant control parameters, Phys. Rev. E **80**, 061905 (2009).
[23] A. Sakashita, N. Urakami, P. Ziherl, and M. Imai, Three-dimensional analysis of lipid vesicle transformations, Soft Matter **8**, 8569 (2012).
[24] B. Bozic and S. Svetina, Vesicle self-reproduction: The involvement of membrane hydraulic and solute permeabilities, Eur. Phys. J. E. Soft Matter **24**, 79 (2007).
[25] J. Macía and R. V. Solé, Protocell self-reproduction in a spatially extended metabolism-vesicle system, J. Theor. Biol. **245**, 400 (2007).
[26] J. Macía and R. V. Solé, Synthetic turing protocells: Vesicle self-reproduction through symmetry-breaking instabilities, Philos. Trans. R. Soc. B Biol. Sci. **362**, 1821 (2007).
[27] A. J. Markvoort, A. Smeijers, K. Pieterse, R. van Santen, and P. Hilbers, Lipid-based mechanisms for vesicle fission, The J. Phys. Chem. B **111**, 5719 (2007).
[28] A. Markvoort, P. Spijker, A. Smeijers, K. Pieterse, R. Van Santen, and P. Hilbers, Vesicle deformation by draining: Geometrical and topological shape changes, J. Phys. Chem. B **113**, 8731 (2009).
[29] A. J. Markvoort, N. Pfleger, R. Staffhorst, P. A. Hilbers, R. A. Van Santen, J. A. Killian, and B. De Kruijff, Self-reproduction of fatty acid vesicles: A combined experimental and simulation study, Biophys. J. **99**, 1520 (2010).
[30] R. Bruckner, S. Mansy, A. Ricardo, L. Mahadevan, and J. Szostak, Flip-flop-induced relaxation of bending energy: Implications for membrane remodeling, Biophys. J. **97**, 3113 (2009).
[31] Y. Sakuma and M. Imai, From vesicles to protocells: The roles of amphiphilic molecules, Life **5**, 651 (2015).
[32] W. Rawicz, K. Olbrich, T. McIntosh, D. Needham, and E. Evans, Effect of chain length and unsaturation on elasticity of lipid bilayers, Biophys. J. **79**, 328 (2000).
[33] M. G. Sacerdote and J. W. Szostak, Semipermeable lipid bilayers exhibit diastereoselectivity favoring ribose, Proc. Natl. Acad. Sci. U.S.A. **102**, 6004 (2005).
[34] K. Olbrich, W. Rawicz, D. Needham, and E. Evans, Water permeability and mechanical strength of polyunsaturated lipid bilayers, Biophys. J. **79**, 321 (2000).
[35] D. Huster, A. Jin, K. Arnold, and K. Gawrisch, Water permeability of polyunsaturated lipid membranes measured by 17O NMR, Biophys. J. **73**, 855 (1997).
[36] M. Jansen and A. Blume, A comparative study of diffusive and osmotic water permeation across bilayers composed of phospholipids with different head groups and fatty acyl chains, Biophys. J. **68**, 997 (1995).
[37] M. M. Kamal, D. Mills, M. Grzybek, and J. Howard, Measurement of the membrane curvature preference of phospholipids reveals only weak coupling between lipid shape and leaflet curvature, Proc. Natl. Acad. Sci. U.S.A. **106**, 22245 (2009).
[38] P. Canham, The minimum energy of bending as a possible explanation of the biconcave shape of the human red blood cell, J. Theor. Biol. **26**, 61 (1970).

[39] O.-Y. Zhong-can and W. Helfrich, Bending energy of vesicle membranes: General expressions for the first, second, and third variation of the shape energy and applications to spheres and cylinders, Phys. Rev. A **39**, 5280 (1989).
[40] See Supplemental Material at http://link.aps.org/supplemental/10.1103/PhysRevLett.123.038102 including Refs. [41–50].
[41] Y. Kim and C. S. Peskin, 2-D parachute simulation by the immersed boundary method, SIAM J. Sci. Comput. **28**, 2294 (2006).
[42] Y. Kim, Y. Seol, M.-C. Lai, and C. S. Peskin, The immersed boundary method for two-dimensional foam with topological changes, Commun. Comput. Phys. **12**, 479 (2012).
[43] Y. Kim, M.-C. Lai, C. S. Peskin, and Y. Seol, Numerical simulations of three-dimensional foam by the immersed boundary method, J. Comput. Phys. **269**, 1 (2014).
[44] Z. Li and M.-C. Lai, The immersed interface method for the Navier-Stokes equations with singular forces, J. Comput. Phys. **171**, 822 (2001).
[45] T. G. Fai, B. E. Griffith, Y. Mori, and C. S. Peskin, Immersed boundary method for variable viscosity and variable density problems using fast constant-coefficient linear solvers I: Numerical method and results, SIAM J. Sci. Comput. **35**, B1132 (2013).
[46] T. G. Fai, B. E. Griffith, Y. Mori, and C. S. Peskin, Immersed boundary method for variable viscosity and variable density problems using fast constant-coefficient linear solvers II: Theory, SIAM J. Sci. Comput. **36**, B589 (2014).
[47] K. A. Brakke, The surface evolver, Exp. Math. **1**, 141 (1992).
[48] M. Botsch, L. Kobbelt, M. Pauly, P. Alliez, B. Levy, L. Kobbelt, M. Pauly, P. Alliez, and B. Levy, *Polygon Mesh Processing* (A.K. Peters/CRC Press, Boca Raton, Florida, 2010).
[49] E. E. Kooijman, V. Chupin, N. L. Fuller, M. M. Kozlov, B. de Kruijff, K. N. J. Burger, and P. R. Rand, Spontaneous curvature of phosphatidic acid and lysophosphatidic acid, Biochemistry **44**, 2097 (2005).
[50] J. D. Weeks, D. Chandler, and H. C. Andersen, Role of repulsive forces in determining the equilibrium structure of simple liquids, J. Chem. Phys. **54**, 5237 (1971).
[51] C. S. Peskin, The immersed boundary method, Acta Numer. **11**, 479 (2002).